The Thermal Unimolecular Decomposition of Methyl Chloride behind Shock Waves

Osamu KONDO, Ko SAITO,* and Ichiro MURAKAMI

Department of Chemistry, Faculty of Science, Hiroshima University, Hiroshima 730

(Received November 22, 1979)

The thermal decomposition of methyl chloride diluted in Ar has been studied behind shock waves over the temperature range between 1680 and 2430 K and the total density range of 2.0×10^{-6}—3.5×10^{-5} mol cm^{-3}. The decomposition rate was monitored by means of the UV absorption of the CH_3 radical produced. The initiation reaction was found to be the C–Cl bond fission; the process proceeded in the fall-off region under the present experimental conditions. From the fall-off data, low- and high-pressure rate constants (k_0/[Ar] and k_∞) were obtained by the application of a refined RRKM theory involving a weak collision effect. Thus, the Arrhenius expressions were given as:

$$k_0/[\mathrm{Ar}] = 10^{15.56}\exp(-247\ \mathrm{kJ\ mol^{-1}}/RT)\ \mathrm{cm^3\ mol^{-1}\ s^{-1}},$$
$$k_\infty = 10^{13.86}\exp(-383\ \mathrm{kJ\ mol^{-1}}/RT)\ \mathrm{s^{-1}}.$$

The collision efficiency factor, β_c, was obtained as 0.02 at the mean temperature of the experiment by comparing the low-pressure rate constant with the strong collision-rate constant. The high-pressure rate constant was well explained by the maximum free-energy criterion presented by Quack and Troe.

The thermal unimolecular decompositions of halomethanes are very interesting in the following points: 1) They are important test cases for the theories of unimolecular reactions; 2) There are two possible reaction channels as the initiation reaction (*i.e.*, simple bond fission and molecular elimination); 3) The pressure dependence of the unimolecular reaction varies depending on the channel and halogen. The thermal decompositions were previously investigated behind shock waves for CHF_3,[1-4] CH_3F,[5] $CHClF_2$,[4] $CHCl_3$,[4,6] and CH_3I.[7] It was found that the decompositions of these molecules are initiated *via* the molecular elimination except for the case of CH_3I. A common feature of these reactions is that the heats of reaction, ΔH_r°, for the molecular eliminations are always substantially lower than that of the simple bond fissions. In most cases, the unimolecular processes of the molecular elimination were in the high- or falloff-pressure regions under the usual shock-wave conditions.[8] According to the experimental results obtained hitherto, the molecular eliminations which have three-center activated complexes have potential barriers above, but not more than 40 kJ mol^{-1}, the heats of reaction. However, for the case of CH_3I, the value of ΔH_r° for the C–I bond fission is rather lower than that of the HI elimination by about 159 kJ mol^{-1}. Moreover, the unimolecular process of this reaction was found in the low-pressure region. The energy-transfer efficiency in the CH_3I–Ar system was found to be very small.

For the case of CH_3Cl, the heats of reaction of the two channels are very close to each other (the ΔH_r° for the C–Cl bond fission is less than that for the HCl elimination by about 25 kJ mol^{-1}). It can, therefore, be expected that the decomposition occurs mainly *via* the C–Cl bond fission, as has been proposed by Shilov and Sabirova,[9] who investigated the pyrolysis in a flow system. If the experimental data for a unimolecular reaction are obtained in a pressure region, it is, in principle, possible to evaluate the rate constants over the whole pressure region involving low- and high-pressure limits by using currently proposed unimolecular theories. Thus, we can discuss, in the high-pressure region, the intramolecular energy distribution and the form of the activated complex, and, in the low-pressure region, the intermolecular energy transfer.

The present paper will report the thermal decomposition of methyl chloride behind shock waves by monitoring the CH_3 behavior. In this work, we could determine high- and low-pressure rate constants from the fall-off data for the primary unimolecular reaction.

Experimental

The experiments have been performed in a shock tube 5 cm in internal diameter. A detailed description of the procedure was given in a previous paper.[10] The UV-absorption system in this work consisted of a deuterium lamp (HTV, L544) as a light source, a monochromator (Jarrell-Ash, 0.25 M), and a photomultiplier (HTV, R106UH). Output signals from the photomultiplier were fed into a pre-amplifier (Iwatsu DA-2A) and then recorded with a transient recorder (Kawasaki Electronica, TM-1410). The resultant rise time of the signal was about 5 μs, enough for the present purposes. The physical properties of the shock-heated gas were calculated from the incident-shock velocity assuming non-reaction conditions. Although relatively high CH_3Cl mixtures (3—5 mol %) were used occasionally, it was considered that the effect of the enthalpy change during the reaction was negligibly small in the early stage of the reaction, from which the rate data were determined.

Methyl chloride (with a 99.5% stated minimum purity) and Ar (99.998%) were used without further purification. Mixtures (0.2—5.0 mol % CH_3Cl in Ar) were prepared in 10-l glass flasks and were allowed to stand for more than 12 h before use. The experimental conditions behind shock waves were as follows: temperature= 1680—2430 K and total density=2.0×10^{-6}—3.5×10^{-5} mol cm^{-3}.

The methyl radical has an absorption band due to the $^2A_1\leftarrow{}^2A_2$ electronic transition which has a maximum at 216 nm.[11] Recent high-temperature measurements of the absorption coefficient at two laboratories have shown a good agreement, within the range of experimental error.[12,13] Glänzer *et al.*[12] determined the absorption coefficient of CH_3 produced from shock-heated azomethane at 216 nm (FWHM=1.6 nm) in the temperature range of 1200—1800 K. Tsuboi[13] also

measured the absorption coefficient at 216 nm (FWHM= 1.4 nm) in a system of ethane–Ar mixtures in the range of 1500—2300 K. Since, in the present study, the absorption measurements were performed at much the same wavelength (FWHM=1.65 nm), it was considered that the absorption coefficient and its temperature dependence reported by the above investigators could be applied to the present analysis of the absorption data without any corrections.

Results

Figure 1 shows a typical absorption record behind reflected shock waves. The absorption intensity begins to increase just behind the reflected shock front and seems to approach a steady value as the reaction proceeds. At the observed wavelength, there is no absorption by the reactant. The products which are considered to have absorptions around 216 nm are C_2H_2, C_2H_3Cl, and HCl, besides the CH_3 radical. The absorption coefficient of C_2H_2 at this wavelength is known to be as small as 1/15 that of CH_3.[13] From the data of the absorption coefficient of C_2H_3Cl at 230 nm ($\varepsilon \simeq 2\times10^5$ cm^2 mol^{-1} at 1600 K),[14] we could estimate that the value at 216 nm is about one-third that of CH_3 at 2000 K. However, since C_2H_3Cl is not the main product, as will be seen later in the computer simulation, its contribution to the absorption profile is negligible. HCl has an absorption band in the vacuum UV region with a maximum at 150—160 nm (ε (160.8 nm)= 1.8×10^6 cm^2 mol^{-1} at 2000 K),[15] while around 200 nm it has a weak absorption which is less than one-tenth the maximum intensity at room temperature.[16] Therefore, the contribution of the HCl absorption to the CH_3 measurement at 216 nm is thought to be negligibly small.

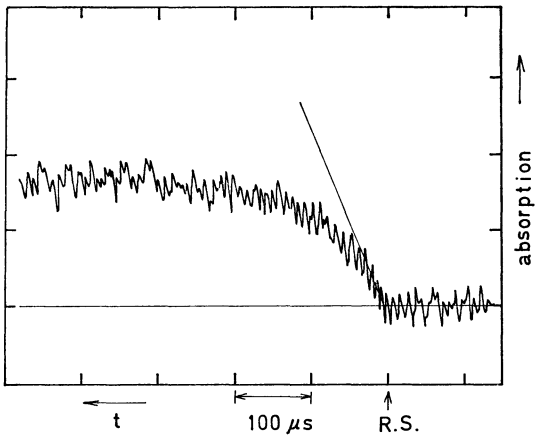

Fig. 1. Typical CH_3 absorption trace at 216 nm during decomposition of CH_3Cl.
T_5=2007 K, $\rho_5=3.52\times10^{-5}$ mol cm^{-3}, 0.5 mol % $CHCl_3$ in Ar. R. S. denotes the reflected shock front.

The initial rate of the CH_3 production was determined by the following relation:

$$\text{Rate} = \{\mathrm{d}[CH_3]/\mathrm{d}t\}_{t=0} = r_0/\varepsilon l$$

$$r_0 = \{\mathrm{d}\ln(I_0/I)/\mathrm{d}t\}_{t=0}$$

where ε is the absorption coefficient; l, the optical path length; I_0, the light intensity of 100% transmission, and

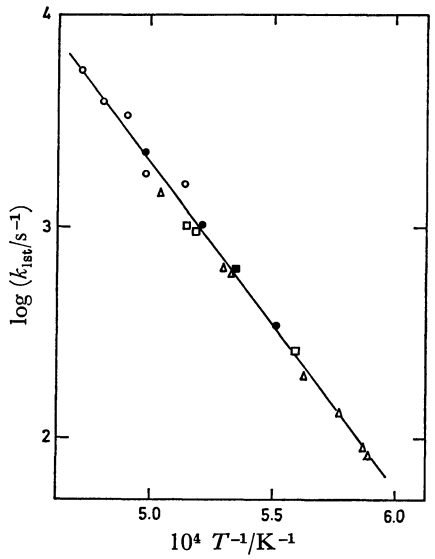

Fig. 2. Arrhenius plot of k_{1st} (initial rate constant of CH_3 production) for different mixtures and at a constant pressure of 5.0 atm (1 atm=101325 Pa).
○: 0.2%, ●: 0.5%, ■: 1.0%, △: 2.0%, □: 2.5%.

I, the intensity of the light that has transmitted the sample gas. In practice, the initial gradient was determined from the initial portion corresponding to the region within about 20% of the steady value. To ascertain the order of the CH_3 production rate with respect to the reactant concentration, the Arrhenius plots of the first-order rate constant, k_{1st}=Rate/$[CH_3Cl]_0$, obtained for various mixtures and at a constant total pressure were made; they are shown in Fig. 2. From this figure it may be seen that k_{1st} does not show any systematic departure from a straight line

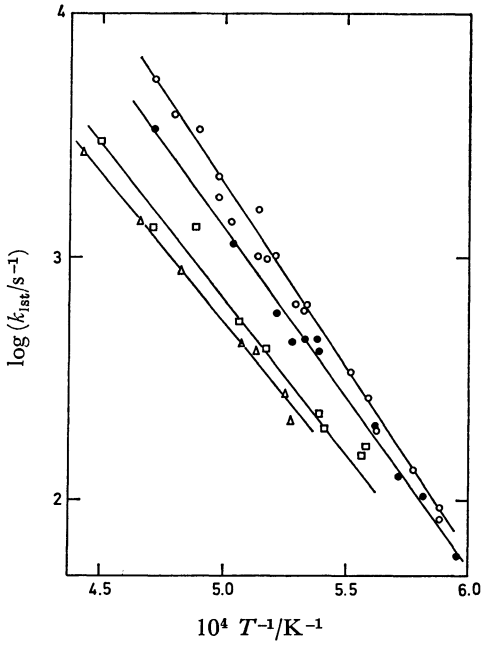

Fig. 3. Arrhenius plots of k_{1st} at different pressures.
Total densities in mol cm^{-3}, averaged over a series of experiments, ○: 3.7×10^{-5}, ●: 1.35×10^{-5}, □: 3.54×10^{-6}, △: 1.99×10^{-6} (incident shock waves).

Table 1. Arrhenius parameters of k_{1st}

Total density / mol cm^{-3}	T / K	A / s^{-1}	E / kJ mol^{-1}
2.0×10^{-6}	1892—2253	8.1×10^{8}	236 ± 4
3.5×10^{-6}	1790—2428	1.9×10^{9}	247 ± 8
1.4×10^{-5}	1678—2119	1.5×10^{10}	269 ± 10
3.7×10^{-5}	1700—2117	8.5×10^{10}	292 ± 14

as the initial concentration of CH_3Cl changes by 12.5-fold. The same results were obtained under the other total pressures adopted. Figure 3 shows a total density dependence of k_{1st}. Also in Table 1 the values of the Arrhenius parameters of k_{1st} are listed for each total density. From Fig. 3 and Table 1 it appears that the apparent first-order rate constants of the CH_3 production are in the fall-off region under the present experimental conditions. In the fall-off region, both the intermolecular energy transfer process and the intramolecular behavior are important equivalently. Thus, it is necessary to evaluate the limiting rate constants for the discussion based on kinetic theories.

Discussion

Reaction Mechanism of the CH_3Cl Decomposition. In the case of methyl chloride, the following two channels are probable for the initiation reactions:

(1) $CH_3Cl\,(+M) \longrightarrow CH_3 + Cl\,(+M)$
$\Delta H^\circ_{r0} = 347$ kJ mol^{-1}

(1a) $CH_3Cl\,(+M) \longrightarrow CH_2 + HCl\,(+M)$
$\Delta H^\circ_{r0} = 372$ kJ mol^{-1}.

Channel 1 has no barrier above the heat of reaction along the reaction coordinate if the potential barrier due to the centrifugal force is neglected. On the other hand, Channel 1a has an activation energy higher than ΔH°_{r0} because, in this channel, a three-center activated complex may be formed during the course of the reaction. Thus, the difference in the activation energies between the two channels becomes larger than the difference in the heats of reaction. Assuming that the values of the preexponential factor are equal, a rough estimation shows that the rate constant, k_{1a}, is smaller than k_1 by several hundredths at 2000 K. Furthermore, in Channel 1a the CH_2 radical produced is the $^3B_1$ state (a spin-forbidden reaction is known to have a small A factor).

A mechanism of the thermal decomposition of methyl chloride has been proposed by Shilov and Sabirova,[9] who investigated the decomposition at around 1100 K and at pressures of 10—15 Torr (1 Torr=133.322 Pa) in a flow system. From the concentration ratios of the products (HCl, CH_4, and C_2H_2), they proposed the following mechanism:

(1) $CH_3Cl \longrightarrow CH_3 + Cl$
(2) $CH_3Cl + Cl \longrightarrow CH_2Cl + HCl$
(3) $CH_3Cl + CH_3 \longrightarrow CH_2Cl + CH_4$
(4) $CH_3Cl + CH_2Cl \longrightarrow CH_2Cl_2 + CH_3$
(7) $2CH_2Cl \longrightarrow C_2H_4Cl_2$
(8) $C_2H_4Cl_2 \longrightarrow C_2H_3Cl + HCl$
(9) $C_2H_3Cl \longrightarrow C_2H_2 + HCl$

To consider the reaction process in further detail, several reactions including reverse reactions must be added to the above mechanism. Thus, we selected the following as probable reactions:

(1) $CH_3Cl\,(+M) \rightleftarrows CH_3 + Cl\,(+M)$
(2) $CH_3Cl + Cl \rightleftarrows CH_2Cl + HCl$
(3) $CH_3Cl + CH_3 \rightleftarrows CH_2Cl + CH_4$
(4) $CH_3Cl + CH_2Cl \rightleftarrows CH_3 + CH_2Cl_2$
(5) $C_2H_6\,(+M) \rightleftarrows 2CH_3\,(+M)$
(6) $Cl_2 + M \rightleftarrows 2Cl + M$

Table 2. Elementary reactions

Reaction	ΔH°_{r298} / kJ mol^{-1}	ΔG°_T / kJ mol^{-1}	Rate constant / cm^3 mol^{-1} s^{-1}	Reference of rate constant
1	347	$-1.381T+358.817$		This work
2	−5.0	$-0.0288T-5.581$	$k_2=10^{13.53}\exp(-14/RT)$	a)
3	−9.2	$17.231\times10^{-4}T-8.7316$	$k_3=10^{10.4}T^{1/2}\exp(-39/RT)$	b)
4	14	$6.887\times10^{-3}T+13.23$		See text
5	369	$-0.164T+372.396$	$k_5=10^{17.11}\exp(-375/RT)$	c)
6	242	$-0.1160T+242.534$	$k_6=10^{13.66}\exp(-190/RT)$	d)
7	−372			See text
8	62.8		$k_8=10^{13.5}\exp(-224/RT)$	e)
9	92.0		$k_9=10^{12.57}\exp(-257/RT)$	f)
10	−376			See text
11	72.0		$k_{11}=10^{13.16}\exp(-236.2/RT)$	g)
12	72.8		$k_{12}=10^{17.41}\exp(-331.7/RT)$	h)

a) T. Fueno, "Chemical Reaction Theory," Asakura-Shoten, (1975). b) F. A. Raal and E. W. R. Steacie, *J. Chem. Phys.*, **19**, 578 (1952). c) J. Troe, "Fifteenth Symposium (Int.) on Combustion," The Combustion Institute, Pittsburgh (1975), p. 667. d) M. van Thiel, D. J. Seery, and D. Britton, *J. Phys. Chem.*, **69**, 834 (1965). e) S. W. Benson and H. E. O'Neal, "Kinetic Data on Gas Phase Unimolecular Reactions," Washington, D.C. (1970). f) F. Zabel, *Int. J. Chem. Kinet.*, **9**, 651 (1977). g) W. Tsang, *J. Chem. Phys.*, **41**, 2487 (1964). h) T. Just, P. Roth, and R. Dumm, "Sixteenth Symposium (Int.) on Combustion," The Combustion Institute, Pittsburgh (1977), p. 961.

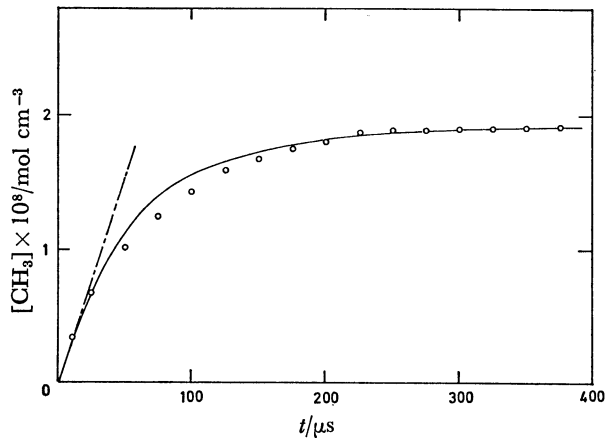

Fig. 4. Comparison of the CH_3 concentration profiles between the calculation (——) and the experiment (○).
T_5=2007 K, $\rho_5=3.52\times10^{-5}$ mol cm^{-3}, 0.5 mol % CH_3Cl in Ar.

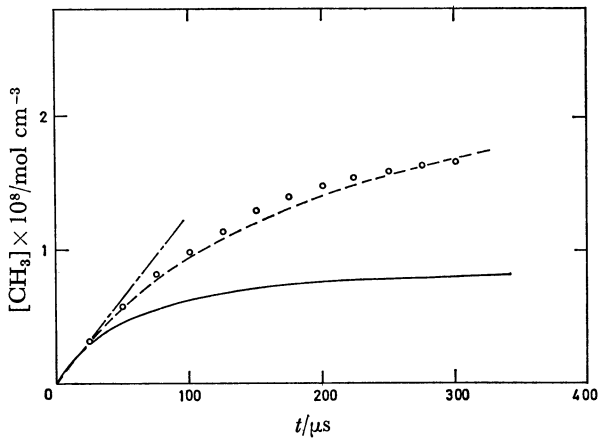

Fig. 5. Comparison of the CH_3 concentration profiles between the calculations (—— and --- , see text) and the experiment (○).
T_5=1730 K, $\rho_5=3.85\times10^{-5}$ mol cm^{-3}, 2.0 mol % CH_3Cl in Ar.

(7) $2CH_2Cl \longrightarrow C_2H_4Cl_2$

(8) $C_2H_4Cl_2 \longrightarrow C_2H_3Cl + HCl$

(9) $C_2H_3Cl\ (+M) \longrightarrow C_2H_2 + HCl\ (+M)$

(10) $CH_2Cl + CH_3 \longrightarrow C_2H_5Cl$

(11) $C_2H_5Cl \longrightarrow C_2H_4 + HCl$

(12) $C_2H_4 + M \longrightarrow C_2H_2 + H_2 + M$

The values of ΔH°_{r298} and ΔG°_T and the rate constants are listed in Table 2. For the present purposes, we need to know how the CH_3 production rate is affected by the secondary reactions. This is important, particularly because we base the decomposition-rate measurement on the initial slope of the CH_3 absorption records. Since there are no available kinetic data for Reactions 4, 7, and 10, we first assumed that Reaction 4 was negligible and that the values of k_7 and k_{10} were equal to the rate constant for the CH_3 recombination. The k_{1st} value corresponding to the total density considered was used as the rate constant of Reaction 1. At 2007 K, a good agreement is seen between the calculation and the observation over the whole range of reaction times, as is shown in Fig. 4. At 1730 K, however, the CH_3 concentration profiles show that the calculation gives a lower steady value, within a shorter reaction time, compared with the observed profile, as is shown in Fig. 5. It was, therefore, necessary to check the rate constants of the reactions which were connected with the CH_3 production. If the alternative reaction channel of the initiation, *i.e.*, Reaction 1a, is considered, a secondary reaction such as (b) $CH_3Cl + CH_2 \rightarrow CH_3 + CH_2Cl$ is needed for the production of the CH_3 radical. An Arrhenius expression of k_b was assumed by the use of the BEBO method[17] and the transition state theory as:

$$k_b = 10^{11.5}\exp\{-(41.8\ \text{kJ mol}^{-1})/RT\}\ \text{cm}^3\ \text{mol}^{-1}\ \text{s}^{-1}.$$

It was ascertained by simulations that the concentration of CH_3 produced by the above reaction was quite low compared with the observed value. Also, it was found that Reaction 5 does not affect the overall reaction profile of CH_3. Thus, it is likely that the computed low values of the steady concentration of CH_3 at lower temperatures are ascribable to the assumption for the k_4, k_7, and k_{10} values. Tentatively, if we use $k_4=10^{11.3}$ cm^3 mol^{-1} s^{-1} and $k_7=k_{10}=10^{11.5}$ cm^3 mol^{-1} s^{-1} at 1730 K, the calculation shows a good agreement with the observed profile (the dotted line in Fig. 5). However, we could not determine a unique set of rate constants which agrees with the profiles obtained over the temperature range and the concentration range employed in this work. Consequently, from the simulation study we found the following facts: (a) At lower temperatures Reaction 4 affects the CH_3 profile seriously, so that it cannot be neglected in considering the reaction mechanism. (b) The recombination reactions 7 and 10 could not be replaced by the recombination rate of CH_3; therefore, they should be evaluated independently. In this respect, it seems unreasonable to use the collision number as the recombination rate constant as in the case of C_2H_5.[18] (c) It was ascertained that the initial slope of the CH_3 production corresponds fairly well to the initiation reaction, *i.e.*, Reaction 1.

Evaluation of Low- and High-pressure Rate Constants.

a. Strong Collision Assumption: In order to evaluate the low- and high-pressure limit rate constants, we first treat the fall-off data on the basis of the strong collision assumption. Figure 6 shows fall-off curves of k_{1st}, with the temperature as a parameter. The solid lines in the figure were calculated by the reduced-form Kassel theory proposed by Troe and Wagner.[19] For the Kassel parameters, S_k and B_k, the definitions as suggested by Troe[20] have been adopted ($S_k=U_{vib}/RT+1=5.4$, 5.5, 5.7, 5.8 and $B_k=B_k(E_0, T, S_k, \nu_i)=15$, 14.5, 14, 13 at 1800, 1900, 2000, and 2100 K respectively, where U_{vib} is the vibrational energy content of CH_3Cl; E_0, the zero temperature activation energy, and ν_i, the vibrational frequencies of CH_3Cl, as taken from Ref. 11. The reduced fall-off curves were obtained using the Kassel integral tables[20] and fitted to the experimental data points in such a way as to meet the following requirements at the same time: (a) The calculated

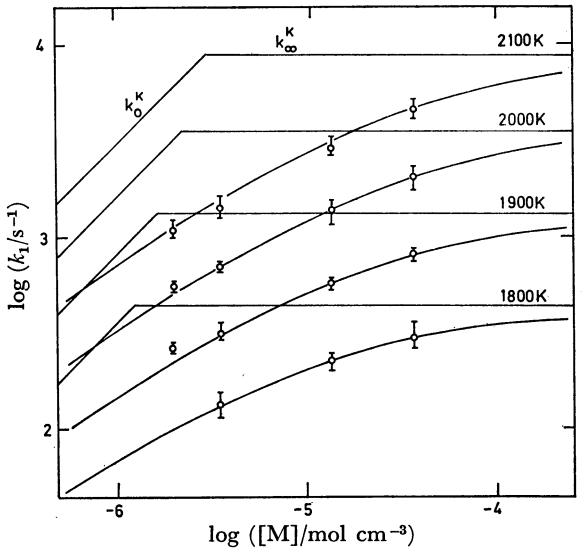

Fig. 6. Pressure dependences of k_{1st} at different temperatures. Full curves are calculated fall-off curves.

curves fit the experimental data points reasonably well, (b) the low- and high-pressure rate constants give temperature-independent activation energies, E_{a0} and $E_{a\infty}$, in the experimental region, and (c) the difference between E_{a0} and $E_{a\infty}$ values obtained is represented approximately by this relation:

$$E_{a\infty} - E_{a0} = (S_{eff}+0.5)R\bar{T},$$

where $S_{eff}=U_{vib}/RT$ and $\bar{T}$ is the mean temperature of the experiments.

The rate constants for the high-pressure limit, k_∞^K, and for the low-pressure limit, k_0^K/[Ar], were then determined at the four temperatures indicated in Fig. 6. Thus, these respective Arrhenius expressions were obtained:

$$k_\infty^K = 10^{11.78}\exp(-315\,\text{kJ mol}^{-1}/RT)\ \text{s}^{-1},$$

$$k_0^K/[\text{Ar}] = 10^{15.08}\exp(-224\,\text{kJ mol}^{-1}/RT)\ \text{cm}^3\ \text{mol}^{-1}\ \text{s}^{-1}.$$

The values of the rate constants evaluated by the above procedure are considered to have an error factor of *ca.* 2.

At first sight, it is likely that the activation energies, $E_{a\infty}$ and E_{a0}, are somewhat lower than those to be expected from the bond-dissociation energy. Also, the preexponential factor of the high-pressure rate constant is considered to be lower than the usual values for the single-bond fission reaction, *i.e.*, $A=10^{13.5\pm1.5}\,\text{s}^{-1}$. In the literature there are experimental results which show somewhat low values for the high-pressure-limit A factor, *e.g.*, $A=10^{11.79}\,\text{s}^{-1}$ for $COF_2\rightarrow COF+F$[21] and $A=10^{12.95}\,\text{s}^{-1}$ for $SF_6\rightarrow SF_5+F$.[22] It is noticable that these experiments were performed in the fall-off region and that the values of the high-pressure rate constant were evaluated by the extrapolation of fall-off curves based on the strong collision assumption. Later Rabinovitch *et al.*[23] corrected the small A factor for the above SF_6 dissociation by considering the weak collision effect to obtain a reasonable value, such as $A=10^{14.11}\,\text{s}^{-1}$. Thus, the above unexpectedly low value of the A factor for $CH_3Cl\rightarrow CH_3+Cl$ may be considered to be the result of the strong collision assumption.

b. Weak Collision Effect on Fall-off Curves: Recently, Luther and Troe[24] published an easy method to obtain a reduced fall-off curve including the weak collision effect. According to this method, the reduced-form rate constant, k/k_∞, is written by the product of three factors as:

$$k/k_\infty = F^{LH}(k_0/k_\infty)F^{SC}(k_0/k_\infty)F^{WC}(k_0/k_\infty) \qquad (I)$$

where $F^{LH}(k_0/k_\infty)$ is a simple Lindemann-Hinshelwood-type fall-off curve, in which the rate constant of the spontaneous reaction, $k(E)$, is independent of the energy,[25a] $F^{SC}(k_0/k_\infty)$ is a factor which includes an energy dependence of $k(E)$,[25b] and $F^{WC}(k_0/k_\infty)$ is a factor pertaining to the weak collision effect.[25c] The parameters used in the calculation of Eq. I are listed in Table 3. Figure 7 shows reduced fall-off curves calculated on the basis of Eq. I. Comparing the two types of fall-off curves in Figs. 6 and 7, it appears that, in the latter, the fall-off region is broad and that the data points fit better than in the former. From the revised fall-off curves in Fig. 7, the high- and low-pressure rate constants are evaluated again, as respectively:

Table 3. Evaluated parameters used for the calculation of k_∞

T/K	S_K	B_K	F^{SC}_{center}	N^{SC}	F^{WC}_{center} a)	N^{WC} a)
1800	5.4	16.1	0.34	1.363	0.63	1.96
1900	5.5	15.6	0.34	1.368	0.62	1.98
2000	5.7	15.5	0.33	1.383	0.62	2.04
2100	5.8	15.1	0.33	1.387	0.62	2.06

a) In the calculations of F^{WC}_{center} and N^{WC}, β_C was taken to be 0.037 at 1800 K (which was the experimental value evaluated from the fall-off curve based on the strong collision assumption) and to have a temperature dependence of $T^{-1.5}$.

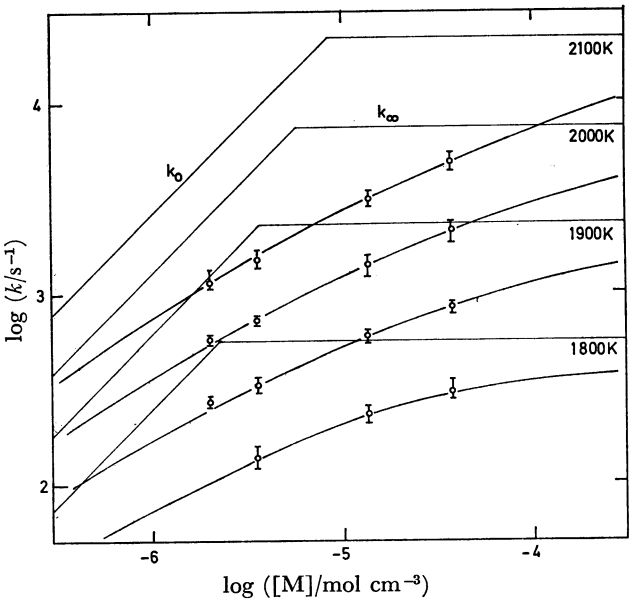

Fig. 7. Fall-off curves computed by considering the weak collision effect.
Data points are the same as in Fig. 6.

$k_\infty = 10^{13.86} \exp(-383\ \text{kJ mol}^{-1}/RT)\ \text{s}^{-1}$,

$k_0/[\text{Ar}] = 10^{15.56} \exp(-247\ \text{kJ mol}^{-1}/RT)\ \text{cm}^3\ \text{mol}^{-1}\ \text{s}^{-1}$.

The error limits involved in these rate constants are considered to be less than a factor of two. It appears that the values of the activation energies and the preexponential factors appearing in the above results are not unexpected when compared with those of other, similar reactions for the single-bond fission.

Calculation of the Unimolecular Rate Constants. In order to ascertain the validity of the high- and low-pressure limit rate constants determined above, it is nescessary to calculate the rate constants theoretically by using currently useful methods. Thus, we will first perform RRKM calculations for the low-pressure rate constant and discuss the intermolecular energy transfer efficiency at high temperatures. Next, we will calculate high-pressure-limit rate constants by evaluating the maximum free energy in the course of the reaction path for the simple bond-fission process.

a. Low-pressure-limit Rate Constant: The theoretical calculation of the low-pressure rate constant was performed by using the appropriate RRKM strong-collision formulation given by Troe:[26,27]

$$k_0^{\text{SC}} = [\text{M}] Z_{\text{LJ}} \rho_{\text{vib}}(E_0) RT Q_{\text{vib}}^{-1} \exp(-E_0/RT) F_{\text{E}} F_{\text{rot}} F_{\text{anh}} \quad \text{(II)}$$

where Z_{LJ} is the Lennard-Jones collision frequency; $\rho_{\text{vib}}(E_0)$, the vibrational energy level density at E_0; E_0, the threshold energy of the reaction; Q_{vib}, the vibrational partition function; F_{E}, the energy dependence of the density of states; F_{rot}, the centrifugal correction factor, and F_{anh}, the anharmonicity factor.[28] The calculation of Eq. II was performed at four different temperatures. The calculated results are listed in Table 4. The molecular constants used in the calculation are shown in the footnote of Table 4.

Actually, at high temperatures the strong collision assumption is not considered to hold; that is, the average energy, $\langle \Delta E \rangle$, which is transferred during collisions between the reactant and the diluent molecule is much lower than RT, the thermal energy of the system. This effect, the weak collision effect, causes a reduction in the apparent reaction rate at high temperatures. The parameter expressing the weak collision effect is defined as the collision efficiency, β_{c}:

$$\beta_{\text{c}} \equiv k_0^{\text{obsd}}/k_0^{\text{SC}} \quad \text{(III)}$$

and:

$$\beta_{\text{c}}/(1-\sqrt{\beta_{\text{c}}}) \simeq -\langle \Delta E \rangle / F_{\text{E}} kT, \quad \text{(IV)}$$

where k_0^{obsd} is the low-pressure-limit rate constant obtained experimentally. The values of β_{c}, F_{E}, and $-\langle \Delta E \rangle/RT$ are also listed in Table 4. The absolute values of β_{c} range between 0.019 and 0.026 in the temperature range studied; this is considered to be reasonable compared with other, similar reactions in Ar (β_{c}=0.015 for CH_3I at 1400 K[7] and β_{c}=0.02 for CH_4 at 2000 K[29]). The temperature dependence of β_{c}, *i.e.*, $\beta_{\text{c}} \propto T^{-2.0}$, is also reasonable when it is compared with theoretical predictions.[30]

It is interesting to compare the value of $-\langle \Delta E \rangle$ evaluated from the experimental data for different reactions in the same diluent gas. For the CH_3I–Ar system, for instance, $-\langle \Delta E \rangle$ ranges from 0.043 to 0.023 in the temperature range of 1100—1500 K.[7] Although the temperature ranges of these systems do not overlap, it appears that the value of $-\langle \Delta E \rangle$ for the CH_3Cl–Ar system is larger than that for the CH_3I–Ar system by a factor of more than two. For the CH_4–Ar system, a value which is comparable to that of the CH_3I–Ar system can be estimated from the data in Ref. 26 ($-\langle \Delta E \rangle/RT$=0.019 at 2000 K). It may be seen that, in the case of the collinear collision of two rigid spheres, the energy-transfer efficiency per collision is largest when the masses of the two spheres are equal.[31] The relative differences in $-\langle \Delta E \rangle$ for the above three systems (*i.e.*, CH_3Cl–Ar > CH_3I–Ar ≅ CH_4–Ar) may be explained, in part, by the relative differences in mass between the reactant and Ar. In this respect, it is also interesting to observe the $-\langle \Delta E \rangle$ values for a given reaction in various diluent gases.

b. High-pressure-limit Rate Constant: A conventional method of estimating the preexponential factor, A, is by the use of the following relation:

$$A = (e\,kT/h) \exp(\Delta S^*/R)$$

ΔS^*, the entropy change of the activation, was evaluated to be 6.7 G mol^{-1}.[32] Consequently, $A = 10^{15.52}\ \text{s}^{-1}$ at 2000 K.

A theoretical prediction of the rate constant for the high-pressure limit may be given by the transition-state formula:[33]

$$k_\infty = (kT/h)(Q^*/Q)$$

where Q and Q^* are the partition functions of the reactant and the activated complex respectively. It is difficult to predict the form of the activated complex precisely although, in a simple bond fission, it does not take so limited a form as a three- or four-center reaction. In this situation, it is considered to be most suitable to apply the method of the maximum free-energy criterion (MFC method) proposed by Quack and Troe[34] for the calculation of Q^*. This method is based on the statistical adiabatic channel model for the activated complex.[35] Strictly speaking, the rate constant calculated with the

Table 4. Values of k_0^{SC}, F_{E}, β_{c}, and $-\langle \Delta E \rangle/RT$

T/K	F_{E}	k_0^{SC} a) / cm^3 mol^{-1} s^{-1}	β_{c}	$\beta_{\text{c}}^{\text{SC}}$ d)	$-\langle \Delta E \rangle/RT$
1800	1.35	9.94×10^9	0.026	0.037	0.042
1900	1.38	2.71×10^{10}	0.023	0.030	0.037
2000	1.41	6.59×10^{10}	0.020	0.025	0.033
2100	1.43	1.44×10^{11}	0.019	0.022	0.032

a) Input data for the calculation of k_0^{SC}: threshold energy, E_0=347 kJ mol^{-1}; Lennard-Jones collision diameter, $\sigma(CH_3Cl\text{–}Ar)$=2.847 Å;[b] Lennard-Jones well depths, $\varepsilon(CH_3Cl)/k$=355 K, $\varepsilon(Ar)/k$=119 K;[b] vibrational frequencies of CH_3Cl, ν/cm^{-1}=732, 2928, 1355, 3047 (2), 1460 (2), 1020 (2).[c] b) J. O. Hirschfelder, C. F. Curtiss, and R. B. Bird, "Molecular Theory of Gases and Liquids," 2nd ed, Wiley, London (1963). c) "JANAF Thermochemical Tables," 2nd ed, Natl. Bur. Stand., (1971). d) $\beta_{\text{c}}^{\text{SC}}$ corresponds to the $k_0^{\text{K}}/k_0^{\text{SC}}$ ratio, where k_0^{K} is the rate constant evaluated by the fall-off curve uncorrected for the weak collision effect.

Table 5. Calculated k_∞^{MFC} values

T/K	γ/Å^{-1} 0	0.75	100	$q^{*a)}$/Å
1800		480[b)]		4.5
1900	40.7	2252	3749.8	4.5
2000	173.7	9059	15200	4.4
2200		98305		4.4

a) q^* is the C–Cl bond distance of the activated complex. b) In s^{-1}.

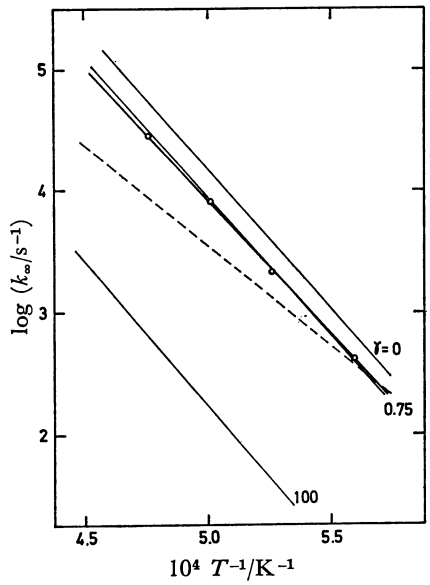

Fig. 8. Comparisons of the high-pressure rate constants. (-○-): k_∞, (------): k_∞^K, (——): k_∞^{MFC}.

MFC method, k_∞^{MFC}, corresponds to the upper limit of the true rate constant.[34] Moreover, the activated complex is defined by the molecular constants of the reactant molecule with only one unknown parameter, γ. Therefore, one could easily calculate the value of Q^* without any large error by using an appropriate γ value. In our calculation, the molecular constants of CH_3Cl and CH_3 were taken from Ref. 11. The C–Cl bond axis was taken as the reaction coordinate. The parameter γ(Å^{-1}) appearing in the equation of the MFC method has the following characteristics: $\gamma=0$ corresponds to the limit of the tight activated complex, and $\gamma=100$, to the limit of the loose activated complex. For many reactions, the calculated values of k_∞^{MFC} are in good agreement with the experimental values when $\gamma=0.75$.[34] In Table 5, the calculated results are listed for $\gamma=0$, 0.75, and 100. In Fig. 8, a comparison is shown between the observed rate constants, k_∞, and k_∞^{MFC}, showing a good agreement when $\gamma=0.75$.

Holbrook[36] analyzed Silov and Sabirova's data and evaluated the rate constants for Reaction 1 as:

$$k_0/[M] = 1.86\times10^4 \text{ cm}^3 \text{ mol}^{-1} \text{ s}^{-1}$$

and:

$$k_\infty = 1.5\times10^{-2} \text{ s}^{-1} \text{ at } 1116.7 \text{ K}.$$

Since the experimental data were near the low-pressure limit, and since he evaluated the limiting values by means of the Hinshelwood plot (*i.e.*, the plot of $1/k$ against $1/P$), the high-pressure value is considered to involve a large error. The extrapolation of the low-pressure rate constant determined in this work leads to $k_0/[Ar]=9.2\times10^3$ cm^3 mol^{-1} s^{-1} at 1116.7 K. Considering that the collision efficiency is large in Shilov and Sabirova's system (M=CH_3Cl), these two experimental values are in good agreement with each other. The value calculated by Forst and St. Laurent[37] is also close to these experimental values.

It was found, in the present study, that the evaluation of the high- and low-pressure-limit rate constants from the fall-off data tends to lead to erroneous results when, especially at high temperatures, the fall-off curve is used without correction for the weak collision effect.

References

1) E. Tschuikow-Roux and J. E. Marte, *J. Chem. Phys.*, **42**, 2049 (1965).
2) E. Tschuikow-Roux, *J. Chem. Phys.*, **42**, 3639 (1965).
3) A. P. Modica and J. E. LaGraff, *J. Chem. Phys.*, **44**, 3375 (1966).
4) K. P. Schug, H. G. Wagner, and F. Zabel, *Ber. Bunsenges. Phys. Chem.*, **83**, 167 (1979).
5) K. P. Schug and H. G. Wagner, *Z. Phys. Chem., N. F.*, **86**, 59 (1973).
6) T. Yano, *Bull. Chem. Soc. Jpn.*, **50**, 1272 (1977).
7) K. Saito, H. Tahara, O. Kondo, T. Yokubo, T. Higashihara, and I. Murakami, *Bull. Chem. Soc. Jpn.*, **53**, 1335 (1980).
8) Exceptionally, in the study of the CHF_3–Ar system by Tschuikow-Roux[2] the unimolecular decomposition to produce CF_2 and HF was found in the low-pressure region under these conditions: 1200 K$\leq T\leq$1800 K, $P\leq$18.7 atm (1 atm=101325 Pa).
9) A. E. Shilov and R. D. Sabirova, *Z. Fiz. Kim.*, **33**, 1365 (1959).
10) T. Higashihara, K. Saito, and H. Yamamura, *Bull. Chem. Soc. Jpn.*, **49**, 965 (1976).
11) G. Herzberg, "Molecular Spectra and Molecular Structure," D. Van Nostrand Co., Princeton, N. J. (1967), Vol. 3.
12) K. Glänzer, M. Quack, and J. Troe, "Sixteenth Symposium (International) on Combustion," The Combustion Institute, Pittsburgh (1977), p. 949.
13) T. Tsuboi, *Jpn. J. Appl. Phys.*, **17**, 709 (1978).
14) F. Zabel, *Int. J. Chem. Kinet.*, **9**, 651 (1977).
15) D. J. Seery and C. T. Bowman, *J. Chem. Phys.*, **48**, 4314 (1968).
16) J. M. Myer and J. A. R. Samson, *J. Chem. Phys.*, **52**, 266 (1970).
17) H. S. Johnston and C. Parr, *J. Am. Chem. Soc.*, **85**, 2544 (1963).
18) A. Lifshitz and M. Frenklach, *J. Phys. Chem.*, **79**, 686 (1975).
19) J. Troe and H. G. Wagner, *Ber. Bunsenges. Phys. Chem.*, **71**, 937 (1967).
20) J. Troe, *Ber. Bunsenges. Phys. Chem.*, **78**, 478 (1974).
21) A. P. Modica, *J. Phys. Chem.*, **74**, 1194 (1970).
22) J. F. Bott and T. A. Jacobs, *J. Chem. Phys.*, **50**, 3850 (1969).
23) B. S. Rabinovitch, D. G. Keil, J. F. Burkhalter, and G. B. Skinner, "Proceedings of the Tenth (International) Shock Tube Symposium," ed by G. Kamimoto, Kyoto (1975),

p. 579.

24) K. Luther and J. Troe, "Seventeenth Symposium (International) on Combustion," The Combustion Institute, Pittsburgh (1979), p. 535.

25) a) The Lindemann-Hinshelwood factor is given by:

$$F^{LH}(k_0/k_\infty) = (k_0/k_\infty)/(1+k_0/k_\infty).$$

b) According to Ref. 24, $F^{SC}(k_0/k_\infty)$ is expressed as:

$$\log F^{SC}(k_0/k_\infty) \frac{\log F^{WC}_{center}}{1+\left\{\frac{\log(k_0/k_\infty)}{N^{WC}}\right\}^2},$$

where F^{SC}_{center}, the broadening factor at the center of the fall-off curve, and the width, N^{SC}, depend on S_K and B_K as:

$$\log F^{SC}_{center} \simeq \frac{0.137(S_K-1)B_K}{1.10(S_K-1)+B_K}$$

and: $N^{SC} \simeq 0.9 - \log F^{SC}_{center}$.

c) $F^{WC}(k_0/k_\infty)$ is expressed as:

$$\log F^{WC}(k_0/k_\infty) \simeq \frac{\log F^{WC}_{center}}{1+\left\{\frac{\log(k_0/k_\infty)}{N^{WC}}\right\}^2},$$

where F^{WC}_{center}, the weak-collision broadening factor at the center of the fall-off curve, depends on β_c, and where the width, N^{WC}, depends on S_K and β_c.

26) J. Troe, *J. Chem. Phys.*, **66**, 4745 (1977).

27) J. Troe, *J. Chem. Phys.*, **66**, 4858 (1977).

28) F_E, F_{anh}, and F_{rot} were calculated by using the approximated equations, (9.9)—(9.12), appearing in Ref. 27.

29) P. Roth and T. Just, *Ber. Bunsenges. Phys. Chem.*, **79**, 682 (1975).

30) There are two opinions regarding the temperature dependence of β_c. Luther and Troe[24] stated that, at the limit of the weak collision, *i.e.*, $-\langle\Delta E\rangle \ll F_E RT$, $\langle\Delta E\rangle$ is constant regardless of the temperature, and that, thus, $\beta_c \propto T^{-1}$. On the other hand Tardy and Rabinovitch (*Chem. Rev.*, **77**, 359 (1977)) proposed $\beta_c \propto T^{-2}$ on the basis of the temperature-independent behavior of $\langle\Delta E\rangle_{down}$, where $\langle\Delta E\rangle_{down}$, the average energy transferred per deactivating collision, is related to $\langle\Delta E\rangle$ as:

$$\langle\Delta E\rangle = -\langle\Delta E\rangle^2_{down}/(\langle\Delta E\rangle_{down}+F_E RT).$$

If $\langle\Delta E\rangle_{down}$ is assumed to be independent of the temperature, the above relation leads to a large drop in β_c at high temperatures.

31) In a collinear collision of the two rigid spheres A and B, the probability of the energy loss of A, R_A, is given by the conservation rules of energy and momentum as:

$$R_A = \frac{4m_A m_B}{(m_A+m_B)^2}\left(1-\frac{v_B}{v_A}\right)\left(1+\frac{m_B v_B}{m_A v_A}\right),$$

where m and v are the mass and the velocity along the collinear axis before collision respectively. It appears from this equation that R_A reaches its maximum when $m_A = m_B$.

32) ΔS^* for each mode is estimated as: ΔS^*(translation)=0; ΔS^*(rotation)=3.6; ΔS^*(symmetry)=0; ΔS^*(internal vibration)=−3.2 (C–Cl stretch)+6.3 (two H–C–Cl bends).

33) S. Glasstone, K. J. Laidler, and H. Eyring, "The Theory of Rate Processes," McGraw-Hill, New York (1941).

34) M. Quack and J. Troe, *Ber. Bunsenges. Phys. Chem.*, **81**, 329 (1977).

35) M. Quack and J. Troe, *Ber. Bunsenges. Phys. Chem.*, **78**, 240 (1974).

36) K. A. Holbrook, *Trans. Faraday Soc.*, **57**, 2152 (1961).

37) W. Forst and P. St. Laurent, *Can. J. Chem.*, **43**, 3052 (1965); **45**, 3169 (1967).